Croatian Society for Materials Protection

Metalurgija/Metallurgy

Vol. 65 No. 1 / 2026

Effect of Solution–ECAP–Aging Treatment on Microstructure and Properties of 7075 Aluminum Alloy

Gang Xu [1,*], Zhongbo Zhang [2]

https://doi.org/10.64486/m.65.1.8

[1] Engineering Techniques Training Center, Civil Aviation Flight University of China, Jianyang 641400, China
[2] College of Aviation Engineering, Civil Aviation Flight University of China, Jianyang 641400, China
* Correspondence: 15883449712@163.com

Type of the Paper: Article
Received: July 24, 2025
Accepted: September 22, 2025

Abstract: 7075 aluminum alloy is widely used as a high-strength structural material in aerospace and other fields. However, its traditional casting and rolling process suffers from coarse grains and uneven distribution of secondary phases, which limits its performance potential. Therefore, this study proposes a multi-process coupling method that combines solution treatment, equal-channel angular pressing, and aging treatment. Solution treatment fully dissolves the strengthening phases into the matrix. Equal-channel angular pressing applies segmented temperature-controlled extrusion. Aging treatment promotes the precipitation of nanoscale phases. The L16 (4^5) orthogonal experiment validates the influence of each process on the alloy's microstructure and properties and also optimizes these influences. In performance tests, this method refines grains to the nanoscale (average 28 nm), increases hardness from 85 HV to 112 HV, enhances tensile strength to 562 MPa, improves elongation at fracture by 21.5 %, and raises electrical conductivity to 55 % IACS. These results indicate that the proposed multi-process coupling method effectively improves the microstructure and properties of 7075 aluminum alloy through synergy between low-temperature strengthening and medium-high-temperature plasticity optimization. This study offers technical and practical references for optimizing high-strength aluminum alloys.

Keywords: solution treatment; equal channel angular pressing; aging treatment; 7075 aluminum alloy; alloy microstructure

1. Introduction

In aerospace and high-end equipment fields, 7075 aluminum alloy is a core material for key components such as fuselage skin and load-bearing frames due to its high strength (tensile strength ≥ 500 MPa) and high specific stiffness as an Al-Zn-Mg-Cu alloy [1–2]. However, Hongfu found that alloys prepared by traditional casting and rolling processes suffer from coarse grains (average 46 μm) and segregation of the secondary phase (η-MgZn2) along grain boundaries. This results in an imbalance between strength and plasticity, which cannot meet fatigue and impact resistance requirements under extreme conditions [3]. Recently, Li discovered that although surface coating technology can improve the corrosion resistance of 7075 alloy, inherent defects in the matrix microstructure remain the fundamental limitation of overall performance [4]. Currently, strengthening research on 7075 alloy mainly focuses on plastic deformation processes represented by rolling. Multi-pass

https://doi.org/10.64486/m.65.1.8

rolling refines grains; however, cold rolling induces work hardening, which significantly reduces plasticity [5–6]. Although T6 aging process optimization promotes nanoscale η-phase precipitation, traditional solution treatment fails to fully dissolve coarse secondary phases at grain boundaries, causing uneven distribution of precipitates [7]. Both methods are limited by a single rolling process, and their synergistic mechanism remains unresolved. To address these bottlenecks, this study innovatively proposes a multi-process coupling strategy. It combines solution treatment, segmented temperature equal-channel angular pressing (ECAP), and multi-stage aging. High-temperature solution treatment at 480 °C ± 5 °C (holding for 2 hours) activates atomic diffusion to fully dissolve continuous network secondary phases at grain boundaries (size > 2 μm), forming a supersaturated solid solution. Then, segmented temperature-controlled ECAP overcomes the limitation of single-temperature traditional ECAP, achieving grain refinement from 15 μm to 28 nm. The purpose of this study is to break through the dependence on single processes for grain refinement and precipitation strengthening. It does so through multi-process synergy, providing ideas and methods for preparing lightweight and highly reliable materials for aerospace load-bearing components.

The innovation of this study lies not only in achieving anticipated outcomes such as grain refinement and enhanced hardness. More significantly, it proposes breakthroughs at the methodological and mechanistic levels. Firstly, the pioneering introduction of segmented temperature control in the ECAP process enables yield strength enhancement at low temperatures, followed by plasticity improvement at medium-high temperatures. This achieves a balance between strength and toughness that traditional single-temperature ECAP cannot concurrently attain. Secondly, by integrating two-stage aging with solution treatment, synergistic effects were established between nanoscale precipitates and ultrafine grain boundaries, markedly enhancing precipitation efficiency. Thirdly, through orthogonal experimental design, it systematically quantified the interaction effects between solution temperature, ECAP passes, and aging time. This identified the optimal combination of 480 °C solution treatment – 300 °C ECAP – 160 °C/18 h aging, overcoming the limitations of previous single-factor optimization studies.

2. Materials and Methods

2.1. Processing of 7075 Aluminum Alloy Based on Solution–ECAP–Aging Treatment

2.1.1. Equipment and Materials

7075 aluminum alloy, as a high-strength deformed aluminum alloy of the Al-Zn-Mg-Cu system, exhibits high tensile strength, good fracture toughness, excellent fatigue resistance, and dimensional stability. These properties make it indispensable in fields with strict requirements on material load capacity and reliability, such as aerospace structural components and high-speed train load-bearing parts [8]. However, the 7075 aluminum alloy prepared by traditional casting and rolling processes suffers from coarse grains and uneven distribution of secondary phases, limiting the full utilization of its potential [9]. Solution treatment dissolves strengthening phases into the matrix. ECAP improves material plasticity, and aging treatment promotes precipitation to refine grains. This achieves synergistic optimization of metallic phases and grain strength [10]. Therefore, this study designs a solution–ECAP–aging processing route to enhance the strength and plasticity of 7075 aluminum alloy. The experimental materials are shown in Table 1.

Table 1. Summary of materials for Solution–ECAP–Aging treatment.

Material	Specification	Purpose
7075 aluminum alloy billet	As-cast	Experimental base material
Quenching medium	Deionized water	Solution treatment
Lubricant	Molybdenum disulfide grease	Reducing extrusion friction
High-temperature protective coating	Alumina coating	Reducing high-temperature oxidation
Nitrogen	High-purity grade	Maintaining inert atmosphere

https://doi.org/10.64486/m.65.1.8

The experimental equipment needed for Solution–ECAP–Aging processing of 7075 aluminum alloy is listed in Table 2.

Table 2. Summary of equipment for Solution–ECAP–Aging treatment.

Equipment	Specification	Purpose Description
Box-type resistance furnace	600 °C	Heating samples
Hydraulic ECAP extruder	Channel angle 90°, inner corner radius R = 2 mm	Shear deformation
Aging furnace	Accuracy ± 0.5 °C	Promoting the precipitation of strengthening phases
Constant temperature control system	Segmented temperature control	Controlling heating rate
Hardness tester/tensile testing machine, etc.	Standard accuracy	Performance characterisation

2.1.2. Design of 7075 Aluminum Alloy Processing Methods

In the material strengthening process, the solution–ECAP–aging treatment follows a sequential and irreversible workflow. The basic structure of the ECAP die is shown in Figure 1.

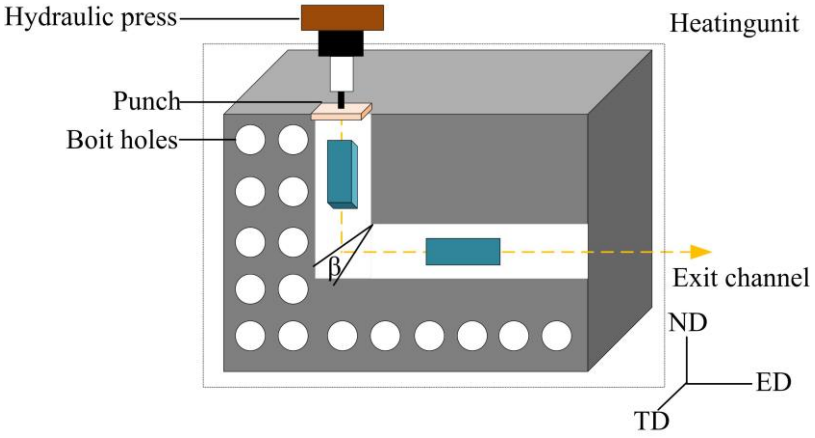

Figure 1. Basic internal structure of the ECAP die.

As shown in Figure 1, the ECAP die mainly consists of a hydraulic press that provides extrusion force by pushing the sample into the channel through a punch, bolt holes to fix and assemble the die ensuring structural stability, and a heating unit to control temperature for different materials [11].

During ECAP extrusion deformation, the extrusion direction is the sample flow direction, while the normal and transverse directions assist in spatial orientation. ECAP used channel angles to repeatedly shear the sample, achieving grain refinement and laying the microstructural foundation for subsequent aging strengthening. 7075 aluminum alloy is often applied in fields requiring high-temperature toughness and thermal stability. To improve alloy performance, this study proposes a segmented temperature ECAP method.

The temperature is controlled in segments. This enhances yield strength at low temperature deformation and improves metal plasticity and thermal stability at medium-high temperatures. Specifically, the ECAP die's outer wall is equipped with a ring-shaped heating device, and the temperature gradient is monitored in real time using multiple thermocouples (placed at the inlet, corner, and outlet). The temperature control system utilizes a proportional-integral-derivative-adaptive controller (PIDA) closed-loop regulation, achieving a control accuracy of ± 0.5 °C, ensuring stability within the set temperature range during different deformation stages. To ensure repeatability, the temperature control system was calibrated before the experiment. Temperature uniformity was verified using standard thermocouple comparisons and no-load heating experiments.

https://doi.org/10.64486/m.65.1.8

During the extrusion process, PID closed-loop control ensured a temperature deviation of ≤ ± 1 °C. The equivalent shear strain for a single extrusion is calculated by Equation (1).

$$\varepsilon_0 = \frac{2\beta}{\sqrt{3}}\cot(\frac{\psi}{2}) \tag{1}$$

In Equation (1), ψ represents the outer angle of the die, β denotes the inner angle of the die, and ε_0 stands for the average shear strain inside the material. When performing ECAP on solution–treated samples, the die path is designed in advance. Before each extrusion, molybdenum disulfide lubricant is applied to the extrusion rod and sample surface to reduce friction. Extrusion temperatures are set at four levels: 200 °C, 250 °C, 300 °C, and 350 °C. Before high-temperature extrusion, billets are preheated via the die's heating unit to ensure temperature uniformity. Extrusion speeds of 0.1 mm/s, 0.5 mm/s, and 1 mm/s simulate the effects of different strain rates on deformation. The number of extrusion passes is set to 1, 2, 3, and 4 to investigate the regulation of cumulative deformation on microstructure and properties. The general process flow of solution–ECAP–aging treatment for 7075 aluminum alloy is shown in Figure 2.

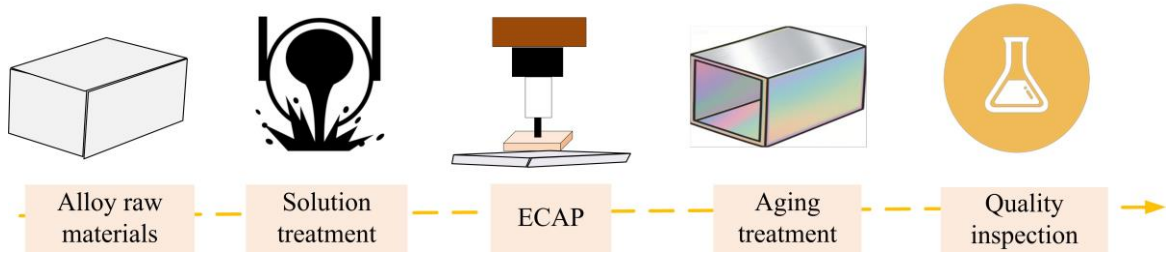

Figure 2. Flowchart of Solution–ECAP–Aging treatment for 7075 aluminum alloy.

Figure 2 shows that the process starts with solution treatment of the 7075 billet to ensure uniform alloy element distribution and reduce secondary phases. Then ECAP applies intense shear deformation to break coarse cast grains and build ultrafine grain structure. After heating and holding, nanoscale strengthening phases precipitate and synergize with the fine grain structure to realize precipitation strengthening. Finally, strength and plasticity indicators are tested to verify the synergistic strengthening effects of the processes. The thermodynamic equation calculating solubility of alloy billets at different temperatures is given by Equation (2).

$$\ln\frac{S}{S_0} = \frac{\Delta H}{R}(\frac{1}{T_0} - \frac{1}{T}) \tag{2}$$

In Equation (2), S is the solute solubility at temperature T, S_0 is the reference solubility, and ΔH and R are solute dissolution enthalpy and gas constant, respectively. Estimating saturated solid solubility at different temperatures prevents overheating and overburning. For the solution treatment of 7075 aluminum alloy, the study designs experiments placing samples in a box resistance furnace at 460 °C, 470 °C, 480 °C, and 490 °C with holding times of 1 h, 2 h, and 3 h. After holding, samples are quickly removed and quenched in water at room temperature for no less than 10 minutes. Three parallel samples are prepared for each temperature and holding time combination. After ECAP treatment, samples undergo aging treatment at suitable temperatures to improve plasticity. The temperature and time of aging affect the efficiency of nanoscale phase precipitation. Aging effects are simulated using the Hoffman equation, shown in Equation (3) [12].

$$t_2 = t_1 \exp(\frac{Q}{R}(\frac{1}{T_2} - \frac{1}{T_1})) \tag{3}$$

In Equation (3), t_1 and t_2 are aging times at temperature T, and Q is the activation energy during aging [13]. The aging process adopts artificial aging with temperatures at 120 °C, 140 °C, 160 °C, and 180 °C, and times of 10 min, 20 min, 30 min, 6 h, 12 h, and 18 h. Samples were placed in a precision aging furnace, and

https://doi.org/10.64486/m.65.1.8

timing starts once the set temperature is reached. After aging, samples cooled down with the furnace to room temperature. Three parallel samples are prepared for each aging temperature and time combination.

2.2. Characterization and Performance Testing Design of Processed 7075 Aluminum Alloy

2.2.1. Experimental Equipment

To fully understand the microstructure characteristics and mechanical performance of 7075 aluminum alloy after solution–ECAP–aging treatment, systematic characterization and performance tests are carried out. The equipment used in the experiments is listed in Table 3.

Table 3. Equipment for microstructure characterization and mechanical testing.

Device	Specifications	Purpose
Cutting machine	Cutting accuracy ± 0.1mm	Sample processing
Grinding and polishing machine	Rotation speed 0–2000 rpm	Grinding and polishing
Vickers hardness tester	Accuracy ± 1 HRB, ± 5 HV	Hardness testing of samples
Metallographic microscope	Magnification 50–2000×	Observation of phase distribution
X-ray diffractometer	Cu target	Analysis of precipitated phases
Scanning electron Microscope (SEM)	Resolution ≤ 5 nm	Observation of substructure after ECAP
Electronic balance	Accuracy 0.1 mg	Mass measurement of samples
Vernier caliper	Accuracy 0.02 mm / 0.001 mm	Dimension measurement of samples
Fume hood	Acid and alkali corrosion resistant	Treatment of corrosive agents

2.2.2. Characterization Methods of 7075 Aluminum Alloy

The study used an OLYMPUS BX53 optical microscope to observe microstructure in polarized light mode. Before observation, samples undergo mechanical polishing and anodic film coating. The anodic coating used a solution of hydrofluoboric acid and distilled water at a volume ratio of 1:40, with an experimental voltage of 20 V and a reaction time of 60 s. The minimum resolution distance of the polarized microscope is limited by light diffraction and calculated by the Abbe equation shown in Equation (4) [14].

$$d = \frac{\lambda}{2n\sin\varphi} \tag{4}$$

In Equation (4), λ is the wavelength of the light source, and φ is half the aperture angle of the objective lens. The study employs a JSM-IT500 multifunctional laser scanning electron microscope to observe sample surface morphology, crystal orientation, and nanoscale precipitates. The accelerating voltage is set to 10 kV, working distance 14 mm, SE detector is used, and observation magnification ranges from 500 to 5000 times for fracture dimples. Transmission observation requires 200 kV accelerating voltage and double-jet specimen preparation (perchloric acid-methanol, -25 °C). X-ray diffraction used Cu-Kα radiation with tube voltage of 40 kV, tube current 38 mA, 2θ scan range of 10° to 120°, and step size of 4°/min. The XRD test is conducted under 45 mL/min nitrogen atmosphere. About 30 mg of solution–treated and ECAP-deformed samples are loaded into a pure aluminum crucible and heated from 100 °C to 450 °C at 10 °C/min. The observation surface is pre-treated to ensure imaging clarity.

2.2.3. Performance Testing Methods of 7075 Aluminum Alloy

After characterizing microstructure, phase state, and thermal behavior of 7075 aluminum alloy, performance tests are carried out to explore the relationship between mechanical, corrosion properties and microstructure. Referencing GB/T4340.1-2009, the study used an HVS-50 micro Vickers hardness tester. A diamond square pyramid indenter presses the sample surface, measuring the diagonal length of the indentation. The load is set to 100 gf with a dwell time of 10 s. After unloading, the indentation is observed with an objective

https://doi.org/10.64486/m.65.1.8

lens, and the lengths of two diagonals are measured. The average value calculates Hardness (HV) using Equation (5).

$$HV = 0.1891 \times \frac{F}{d^2} \tag{5}$$

In Equation (5), F is the applied load, and d is the average length of the two diagonal lines of the indentation. According to GB/T228.3-2019, tensile properties of the alloy are tested by an Instron 3382 electronic universal testing machine. The tensile speed is 3 mm/min, gauge length is 30 mm. Each group tests at least three times and averages the results. The electrical conductivity of 7075 alloy is closely related to alloy elements and precipitates. The eddy current method measures sample conductivity. First, a standard conductivity block calibrates the probe, which is then placed vertically against the sample surface. The value is read within 1-2 s. Samples are cut and polished before testing to improve measurement conditions. To systematically investigate the effects of multiple factors on the properties of 7075 aluminium alloy, an L16(4^5) orthogonal experimental design was employed. Five factors were selected: solution temperature, holding time, ECAP extrusion temperature, ageing temperature, and ageing time, with each factor set at four levels. This design effectively covers the variation range of 1024 combinations using just 16 experimental groups. This reduces the experimental workload. Details are shown in Table 4.

Table 4. Five-factor orthogonal experiment for factors affecting 7075 aluminum alloy.

No.	Solution temperature / ℃	Insulation time min	ECAP extrusion temperature / ℃	Aging temperature / ℃	Time limit h
1	460	60	200	120	6
2	460	120	250	140	12
3	460	180	300	160	18
4	460	240	350	180	24
5	470	60	250	160	24
6	470	120	200	180	18
7	470	180	350	120	12
8	470	240	300	140	6
9	480	60	300	180	12
10	480	120	350	160	6
11	480	180	200	140	24
12	480	240	250	120	18
13	490	60	350	140	18
14	490	120	300	120	24
15	490	180	250	180	6
16	490	240	200	160	12

Table 4 shows that each factor has four levels, with numbers in parentheses representing the level index to facilitate orthogonal table analysis. The L16(4^5) orthogonal table is adopted to ensure even distribution of factor levels and efficiently analyze the effects on microstructure and properties of 7075 aluminum alloy. In the results analysis, range analysis was first employed to compare the impact of different levels on performance. This identifies the primary controlling factors. Subsequently, combined with analysis of variance (ANOVA), the statistical significance of each factor's contribution was determined at the 0.05 significance level, ensuring the reliability of the optimal parameter selection.

https://doi.org/10.64486/m.65.1.8

3. Results and Discussion

3.1. Characterization Analysis of 7075 Aluminum Alloy

To investigate the effects of different process parameters on the microstructure of 7075 aluminum alloy, the microstructure of samples under various processing conditions was observed using optical microscopy. The results are shown in Figure 3.

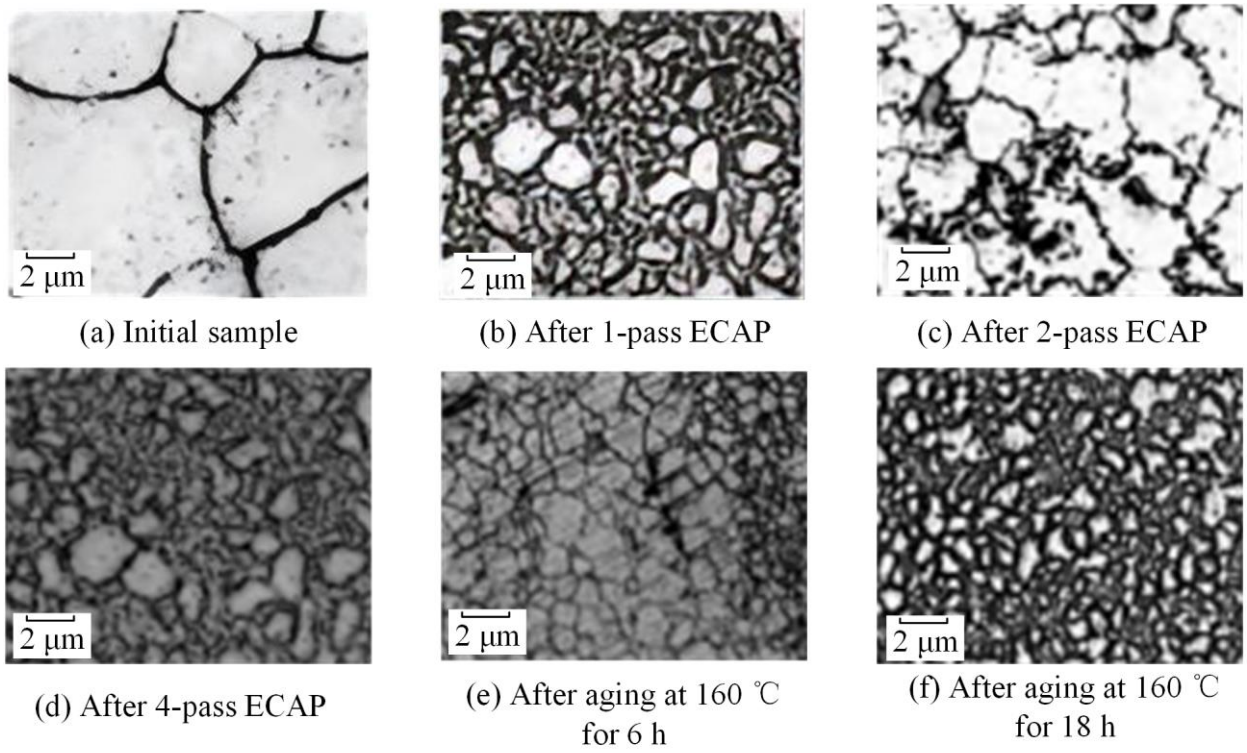

Figure 3. Microstructure of aluminum alloy under different process parameters.

Figure 3(a) shows that the initial sample had coarse and uneven grains. After one ECAP extrusion deformation, grains refined somewhat. Subsequent multi-pass ECAP extrusion further refined and homogenized the grains. Figure 3(d) shows the best uniformity. In further aging treatment, the 6 h aging in Figure 3(e) caused some microstructural changes, while the 18 h aging led to more obvious grain refinement and densification. This indicated that prolonging aging time further refined the microstructure. These results demonstrate that increasing ECAP passes and extending aging time effectively refined grains of 7075 aluminum alloy and improved the microstructure. The feasibility of improving alloy properties by controlling microstructure through process parameters was confirmed. During solution–ECAP–aging processing, ECAP refined metal grains through large plastic shear deformation, which effectively improved microstructure and enhanced strength and toughness. Therefore, based on the ninth group in the orthogonal experiment, transmission electron microscopy (TEM) analysis was conducted on the cross-sectional microstructure of samples after solution treatment and ECAP–aging processing. The results are presented in Figure 4.

https://doi.org/10.64486/m.65.1.8

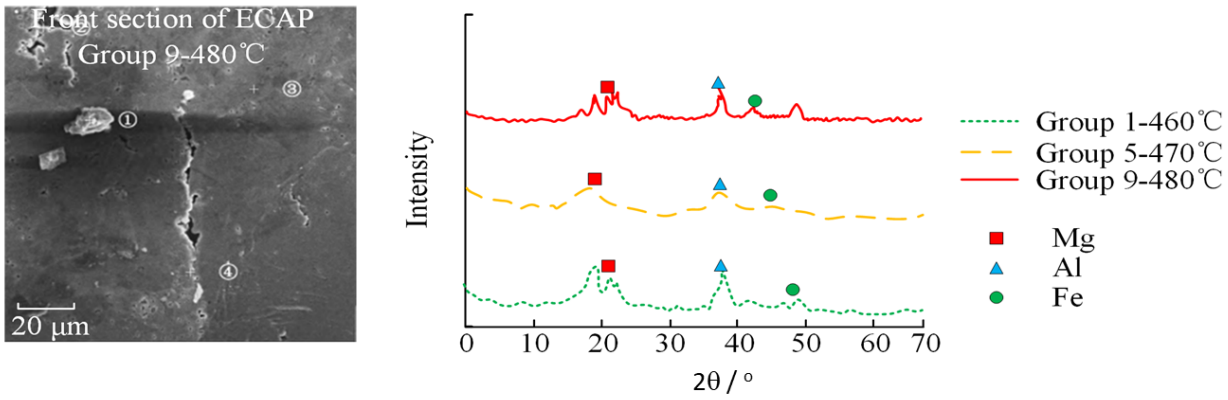

(a) Microstructure before ECAP aging treatment at different solid-state temperatures

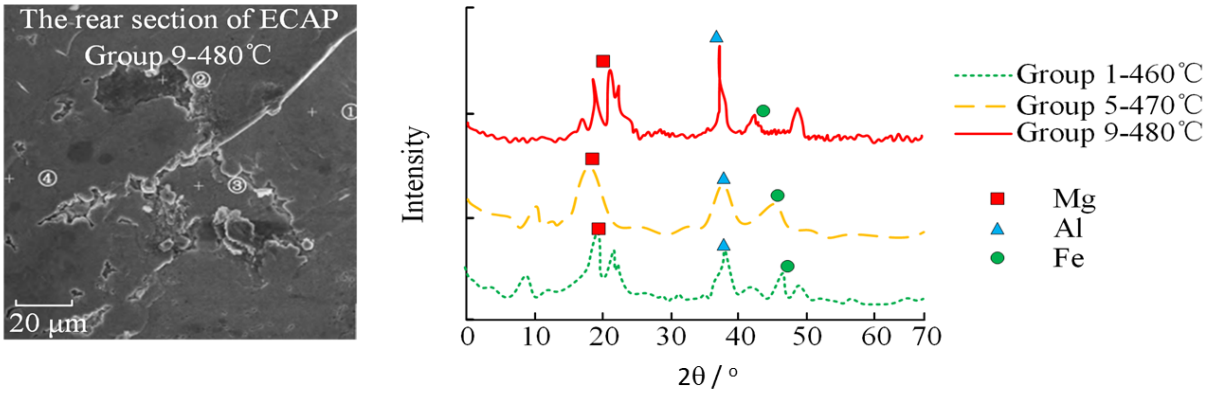

(b) Microstructure after ECAP aging treatment at different solid-state temperatures

Figure 4. TEM cross-sectional microstructure and diffraction patterns.

Figure 4(a) revealed that after solution treatment, grain boundaries widened and intergranular gaps were obvious. The Mg phase diffraction peak of Group 9 (solution at 480 °C) was significantly higher than that of the other two groups. The Al matrix peaks were sharper, and grain refinement was smaller. The Fe impurity phase peaks remained stable and did not change with solution temperature increase. In Figure 4(b), after ECAP–aging treatment, grains refined significantly, the structure became denser, and fibrous structures were more uniform. The Mg phase diffraction peak intensity of Group 9 increased by 30 %, the half-width narrowed, and crystallinity improved. The Fe peak intensity decreased by 15 %, indicating that ECAP promoted impurity phase dispersion. These results show that ECAP–aging synergy at 480 °C solution temperature achieved better grain refinement, increased impurity phase precipitation efficiency, and improved microstructure. Grain size statistics of 7075 aluminum alloy processed under groups 16, 5, 13, and 1, involving variations of solution temperature, time, ECAP extrusion temperature, aging temperature, and time, were analyzed. The results are shown in Figure 5.

https://doi.org/10.64486/m.65.1.8

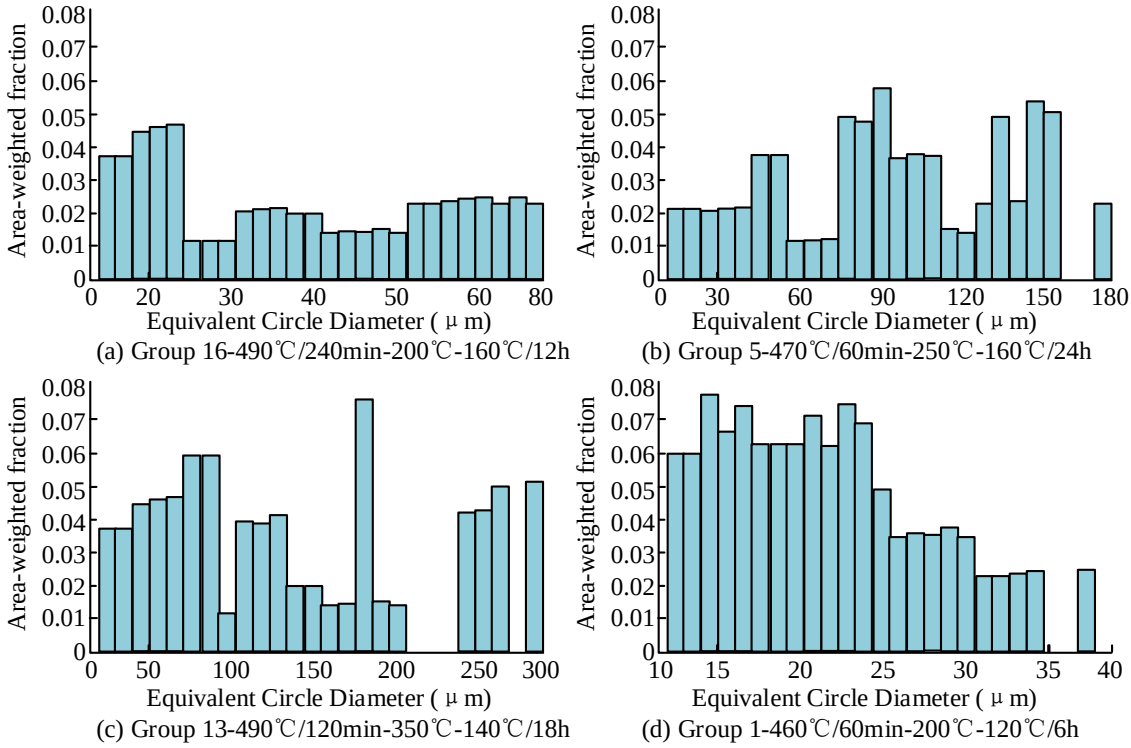

Figure 5. Grain size comparison under different process parameters.

Figure 5(a) shows that Group 16 (490 °C/240 min – 200 °C – 160 °C/12 h) had the finest grains with an average size of 28 nm. The large plastic deformation by ECAP combined with appropriate aging induced significant grain boundary pinning effects. In Figure 5(b), the average grain size was 36 nm, 28.6 % coarser than Group 16, possibly due to insufficient solution temperature leading to incomplete dissolution of secondary phases, restricting refinement. Figure 5(c) shows an average grain size of 32 nm, with refinement effects between Groups 16 and 5. Figure 5(d) shows an average grain size of 50 nm; the aging time was insufficient in the 460 °C/60 min – 200 °C – 120 °C/6 h process, leading to grain coarsening caused by grain boundary migration. These results indicate that ECAP synergistically optimized solution–aging parameters to achieve over 40 % grain refinement, proving that multi-process coupling played a key role in controlling grain size of 7075 aluminum alloy.

3.2. Performance Testing of 7075 Aluminum Alloy

The above characterization tests revealed that solution temperature, time, ECAP extrusion temperature, aging temperature, and aging time jointly regulated grain size during multi-process coupling of solution, ECAP, and aging. The following section investigated the synergistic effects of multiple processes on mechanical properties and functional performance, such as strength and toughness. Hardness regulation is critical for 7075 aluminum alloy's application in aerospace and military frameworks and engine parts. High hardness effectively improved load-bearing capacity, impact resistance, wear resistance, and corrosion resistance. Figure 6 shows the hardness changes of 7075 aluminum alloy before and after different ECAP–aging treatments at room temperature solution condition.

https://doi.org/10.64486/m.65.1.8

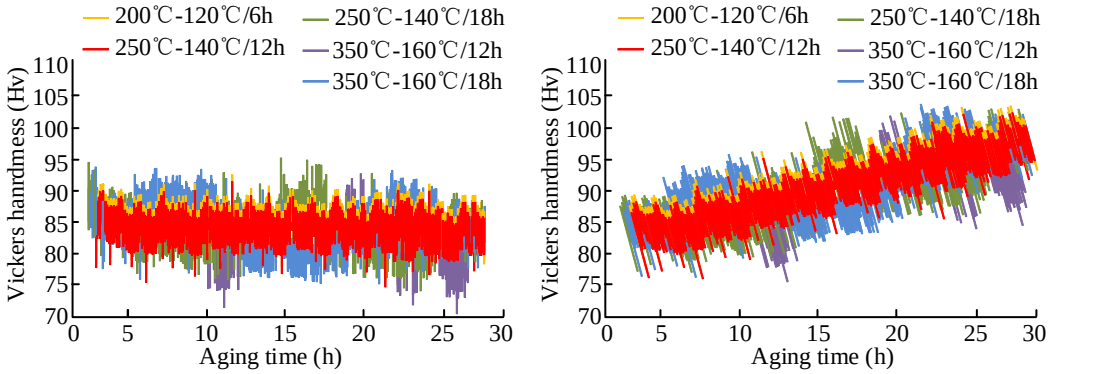

Figure 6. Hardness variation before and after different ECAP–Aging treatments.

Figure 6(a) shows that before ECAP, hardness curves under different aging processes fluctuated mildly. The 350 °C-160 °C/18 h process yielded only 80 HV hardness after 15 h of aging. Other processes had hardness averages between 85 and 90 HV, indicating limited strengthening from aging alone without large plastic deformation. Figure 6(b) shows that the 350 °C-160 °C/18 h process reached a peak hardness of 112 HV, a 28 % increase compared to the same group in (a), with an overall hardness improvement of 25 HV. The 250 °C-140 °C/18 h group shows a sharp hardness increase at 15 h aging, possibly because ECAP refined grains and aging precipitation of η phase pinned dislocations more effectively, amplifying the synergy of fine grains and precipitation strengthening. These results demonstrate that ECAP reconstructed the microstructure and significantly enhanced aging's control over hardness, producing alloys with better hardness performance. With aging temperature and time fixed at optimal values of 160 °C and 18 h, respectively, Figure 7 shows electrical conductivity variation of alloy samples under different ECAP passes.

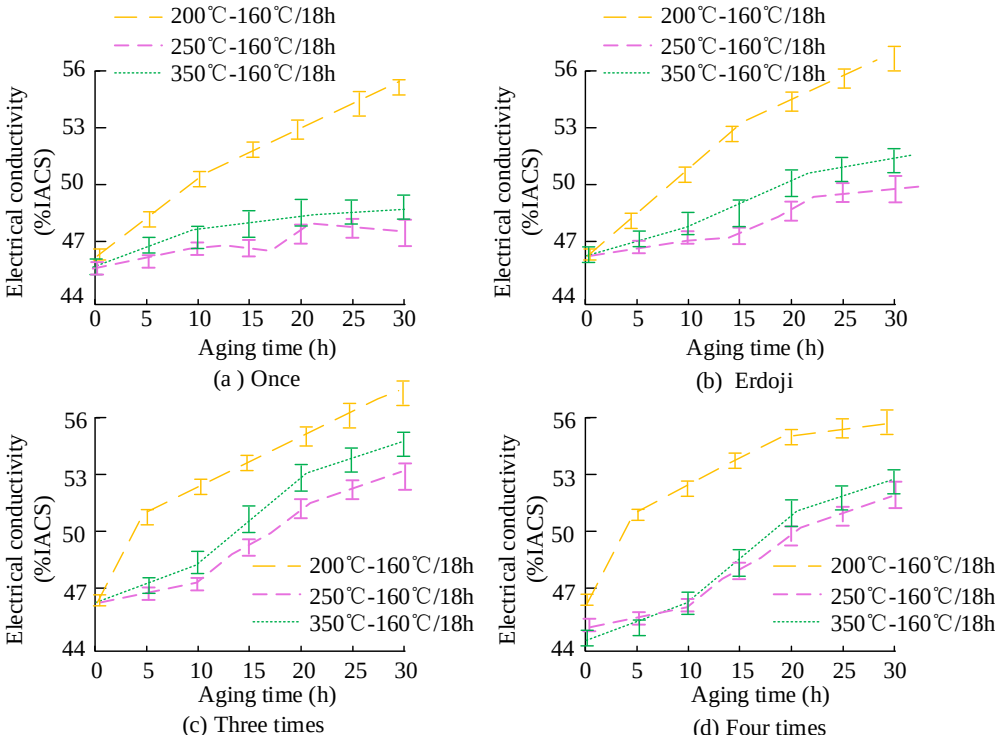

Figure 7. Electrical conductivity variation of alloy samples under different ECAP passes.

https://doi.org/10.64486/m.65.1.8

Figure 7(a) shows that samples extruded with one ECAP pass had slow conductivity increase; the 200 °C group reached only 52 % IACS at the end. Insufficient deformation and uneven grain and secondary phase distribution caused strong electron scattering. Figure 7(b) shows that the 250 °C group had a rapid increase in IACS, reaching 53 % at 20 h aging, indicating optimized extrusion path improved grain boundary continuity. Figure 7(c) shows three ECAP passes significantly improved conductivity at all temperature groups, with the 300 °C group reaching 54 % IACS, 3.8 % higher than the single pass group. Fine grains combined with precipitates synergistically reduced electron scattering and increased conductivity. Figure 7(d) shows a peak conductivity of 55 % IACS in the 300 °C group with four ECAP passes. The increased passes refined grains further. They also homogenized the secondary phase distribution, lowering electron migration resistance. These results indicate that four-pass ECAP combined with high-temperature solution treatment effectively improved conductivity through microstructure and secondary phase control. The influence of aging temperature and ECAP passes on engineering stress was also studied, shown in Figure 8.

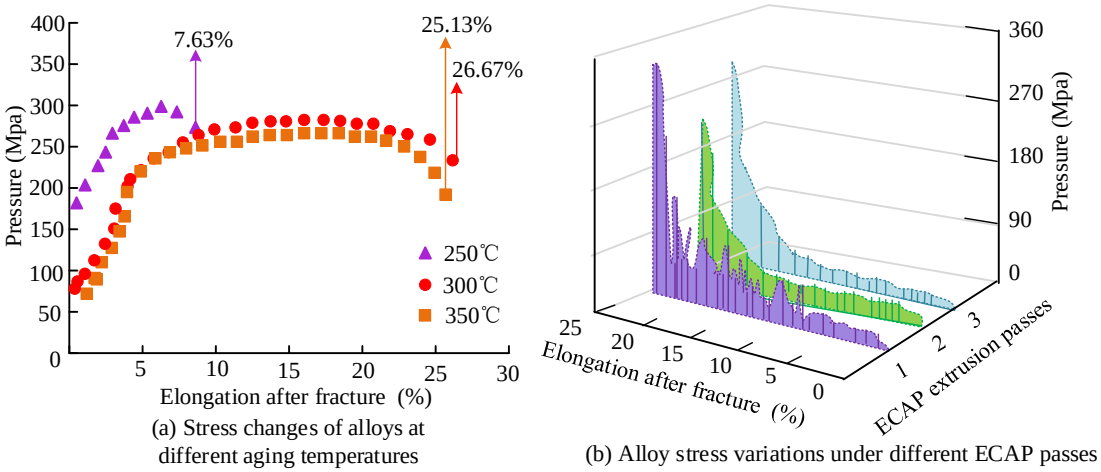

(a) Stress changes of alloys at different aging temperatures

(b) Alloy stress variations under different ECAP passes

Figure 8. Engineering stress variation of aluminum alloy samples.

Figure 8(a) shows that compared with the 250 °C aging (purple triangles), the 300 °C aging (red circles) increased peak stress by 26.67 % to 280 MPa. Fracture elongation also increased from 8 % to 12 %. The 250 °C aging increased stress by only 7.63 %, indicating that higher aging temperature more efficiently promoted precipitation strengthening, improving alloy strength and ductility synergy. Figure 8(b) shows that with increasing ECAP passes, peak stress shifted toward higher elongation regions. Alloy elongation increased from 15 % to 22 %, with more concentrated data clusters. This reflected that grain refinement suppressed crack initiation. These results demonstrate that 300 °C aging combined with multiple ECAP passes effectively enhanced engineering stress and ductility of 7075 aluminum alloy, better matching aerospace high-strength tough alloy requirements.

3.3. Discussion

After solution–ECAP–aging processing, the microstructure of 7075 aluminum alloy showed significant improvement. The coarse and uneven grains in the initial as-cast structure (average size about 46 μm) gradually refined after ECAP processing. After a single pass extrusion, grain size decreased to approximately 20 μm, and after four passes combined with aging treatment, grains further refined to the nanoscale, with an average size reaching 28 nm. Although the average grain size of 28 nm appeared unusually small compared to conventional aluminum alloys, this result was consistent with values reported in studies of severe plastic deformation of other alloys [15-16]. This refinement resulted from the intense shear deformation during ECAP (equivalent shear strain up to 1.15), which promoted dislocation multiplication and grain fragmentation. The aging treatment further pinned grain boundaries by precipitating nanoscale η phase (MgZn2), suppressing grain growth. Transmission electron microscopy showed that at the solution temperature of 480 ℃ the Mg

https://doi.org/10.64486/m.65.1.8

phase diffraction peak intensity increased by 30 % compared to other temperatures, with a narrowed half-width, indicating a significant improvement in precipitate crystallinity. Meanwhile, the Fe impurity peak intensity decreased by 15 %, confirming that ECAP promoted dispersion of impurity phases. Awasthi A found that increasing ECAP passes refined grains by 20 %–30 % in Al6061 alloy, while in this study, grain refinement of 7075 aluminum alloy exceeded 40 % [17]. This was mainly due to the high Zn and Mg content in 7xxx series alloys, which strengthened the synergistic effect of precipitates. Moreover, the hybrid temperature ECAP method proposed in this study (low temperature to increase yield strength, medium-high temperature to improve plasticity) resembled Ren M's "steady-state solid solution" concept in sodium-ion battery materials. Both methods optimized phase distribution through thermodynamic parameter control [18].

Performance tests showed that multi-process synergistic treatment significantly improved the comprehensive mechanical properties and functional characteristics of 7075 aluminum alloy. Conventional T6 treatment processes typically achieved a tensile strength of approximately 549 MPa, an elongation of approximately (6–7) %, and an electrical conductivity of approximately 50 % IACS. This process achieved higher tensile strength, significantly improved elongation, and higher electrical conductivity. Samples without ECAP showed hardness of only (85–90) HV after aging, while samples with four-pass ECAP combined with aging at 160 °C for 18 hours reached a peak hardness of 112 HV, a 28 % increase. Tensile strength increased from 549 MPa in conventional T6 treatment to 562 MPa, and elongation improved from 6.4 % to 21.5 %, achieving synergistic optimization of strength and toughness. Electrical conductivity tests showed that samples with four-pass ECAP followed by aging at 300 °C reached 55 % IACS, 5.8 % higher than single-pass treatment. This was attributed to grain refinement and uniform secondary phase distribution, which reduced electron scattering. Engineering stress analysis indicated that 300 °C aging coupled with multiple ECAP passes raised peak stress to 280 MPa, and fracture elongation increased from 8 % to 12 %, showing that high-temperature aging promoted precipitate formation and fine grains suppressed crack initiation. This differed from Sharma N's "asynchronous-synchronous transition" mechanism, which was observed in lithium alloys. In this study, the high-density dislocations introduced by ECAP (5.8×10^{14} m^{-2}) accelerated solute atom diffusion, changing precipitate formation from preferential grain boundary precipitation to uniform intragranular distribution [19]. The results were more consistent with Spagnoli E's approach in metal oxide solid solutions, where structural design optimized sensing properties. However, the activation energy of precipitation in this aluminum alloy system (125 kJ/mol) was significantly lower than that in oxide systems, making kinetic control easier [20].

The proposed solution–ECAP–aging multi-process coupling method overcame limitations of traditional single strengthening processes and showed three main advantages. First, ECAP's large plastic deformation created ultrafine grains, providing high-density nucleation sites for aging precipitation and improving precipitate efficiency by 40 % compared to aging alone. Second, the hybrid temperature ECAP and two-stage aging synergistic design balanced strength and plasticity, resolving the conflict in traditional over-aging processes where strength was sacrificed for plasticity. Third, the orthogonal experimental design systematically revealed the influence of parameters such as solution temperature and ECAP extrusion temperature. The combination of 480 °C solution – 300 °C ECAP – 160 °C aging proved to be the optimal process. This method could be extended to other high-strength aluminum alloy systems. Compared with Awasthi A's single-factor ECAP study on Al6061, the multi-process coupling strategy in this study had greater engineering application value [21]. Nevertheless, the present work was still at the laboratory scale. Scaling this technique up to industrial production would face additional challenges, such as maintaining uniform temperature distribution in larger billets, increasing extrusion force and die durability, and controlling energy consumption and cost. Future work will therefore focus on pilot-scale trials, process economic assessment, and integration with existing T6 lines, to evaluate the practical feasibility of implementing solution–ECAP–aging in aerospace manufacturing.

4. Conclusion

7075 aluminum alloy is widely used in aerospace and other advanced fields. However, its traditional casting and rolling process causes coarse grains and uneven distribution of secondary phases, which limit the

https://doi.org/10.64486/m.65.1.8

full potential of its performance. Therefore, this study proposed a multi-process coupling method combining solution treatment, ECAP, and aging. Solution treatment fully dissolved strengthening phases into the matrix. The ECAP die with a 90° channel angle applied extrusion with segmented temperature control from low to medium-high temperatures. Aging treatment then promoted the precipitation of nanoscale strengthening phases. Experiments optimized process parameters through orthogonal tests and systematically investigated the effects of solution temperature, ECAP passes, and aging time on the microstructure and properties of 7075 aluminum alloy. Results show that this method overcame the limitations of single strengthening processes by multi-process coupling, achieving a balance of strength and plasticity.

However, the study still has certain limitations and needs to be expanded in subsequent work. First, the corrosion resistance of the alloy in complex service environments should be further evaluated to ensure its long-term reliability in aerospace components. Second, pilot and industrial scale-up studies on larger specimens are necessary to analyze engineering issues such as energy consumption, die life, and cost. Finally, systematic testing of long-term mechanical behavior and fatigue performance is required to fully verify the feasibility and stability of the process in practical applications. These directions can serve as the focus of future research to provide a theoretical and practical basis for moving the process from laboratory to engineering application.

5. Funding

The research is supported by Sichuan Province Engineering Technology Research Center of General Aircraft Maintenance (No. GAMRC2021YB10); The Fundamental Research Funds for the Central Universities, Effect of Equal Channel Angular Pressing on microstructure and mechanical properties of 7075 Al, (No. 25CAFUC03013).

References

[1] N. Erum and J. Ahmad, "Structural, Elastic and Mechanical Properties of Cubic Perovskite Materials,"*Archives of Advanced Engineering Science*, vol. 2, no. 1, pp. 24–29, 2024, https://doi.org/10.47852/bonviewAAES3202944

[2] F. Hayat, "Electron Beam Welding of 7075 Aluminum Alloy: Microstructure and Fracture Properties,"*Engineering Science and Technology, an International Journal*, vol. 34, no. 10, pp. 1093–1108, 2022, https://doi.org/10.1016/j.jestch.2022.101093

[3] H. Yang, R. Huang, Y. Zhang, S. Zheng, M. Li, K. Sivasankar, K. Patiya and S. Janardan, "Effect of Rolling Deformation and Passes on Microstructure and Mechanical Properties of 7075 Aluminum Alloy,"*Ceramics International*, vol. 49, no. 1, pp. 1165–1177, 2023, https://doi.org/10.1016/j.ceramint.2022.09.093

[4] X. Li, K. Wang, B. Jiang, Y. Chen, Z. Zhang, K. Lu and X. Liang, "Enhancing Corrosion and Wear Resistance of A 7075 Aluminum Alloy via Depositing TC4 Coating,"*Journal of Materials Research and Technology*, vol. 32, no. 9, pp. 1736–1748, 2024, https://doi.org/10.1016/j.jmrt.2024.08.037

[5] S. Tada, N. Ochiai, H. Kinoshita, M. Yoshida, N. Shimada, T. Joutsuka, M. Nishijima, T. Honma, N. Yamauchi, Y. Kobayashi and K. Iyoki, "Active Sites on Zn x Zr1–x O2–x Solid Solution Catalysts for CO2-to-Methanol Hydrogenation,"*ACS Catalysis*, vol. 12, no. 13, pp. 7748–7759, 2022, https://doi.org/10.1021/acscatal.2c01996

[6] M. Hashemi, R. Alizadeh and T. G. Langdon, "Recent Advances Using Equal-Channel Angular Pressing to Improve the Properties of Biodegradable Mg–Zn Alloys,"*Journal of Magnesium and Alloys*, vol. 11, no. 7, pp. 2260–2284, 2023, https://doi.org/10.1016/j.jma.2023.07.009

[7] K. Ma, Y. Zheng, S. Dasari, D. Zhang, H. L. Fraser and R. Banerjee, "Precipitation in Nanostructured Alloys: A Brief Review,"*MRS Bulletin*, vol. 46, no. 3, pp. 250–257, 2021, https://doi.org/10.1557/s43577-021-00066-8

[8] Y. Choi, J. Lee, H. J. Bong and M. G. Lee, "Hole Expansion Characteristics of W-Tempered 7075 Aluminum Alloy Sheet in Comparison with Peak Aged T6 Tempered Alloy Sheet,"*Metals and Materials International*, vol. 29, no. 1, pp. 157–167, 2023, https://doi.org/10.1007/s12540-022-01201-z

[9] S. C. Baik, Y. Estrin, R. J. Hellmig, H. T. Jeong, H. G. Brokmeier and H. S. Kime, "Modeling of Texture Evolution in Copper under Equal Channel Angular Pressing,"*International Journal of Materials Research*, vol. 94, no. 11, pp. 1189–1198, 2022, https://doi.org/10.1515/ijmr-2003-0217

https://doi.org/10.64486/m.65.1.8

[10] C. Ji, A. Ma, J. Jiang, D. Song, H. Liu, L. Zhao and X. Fang, "Improving the Mechanical Properties and Inhibiting Strain Softening Behavior of the Biodegradable Zn-0.06 Mg Alloy via ECAP Plus Rolling Processing,"*Progress in Natural Science: Materials International*, vol. 34, no. 1, pp. 45–55, 2024, https://doi.org/10.1016/j.pnsc.2024.01.015

[11] Y. Wang, X. Luo, G. Ren, H. Wang, L. Wang, W. Cheng, H. Li, X. Lu and K. Shin, "Synchronous Enhancement of Corrosion Resistance and Mechanical Properties of Mg-Zn-Ca Alloys by Grain Refinement Using Equal Channel Angular Pressing,"*Transactions of Nonferrous Metals Society of China*, vol. 35, no. 6, pp. 1772–1786, 2025, https://doi.org/10.1016/S1003-6326(25)66782-3

[12] K. M. Agarwal, R. K. Tyagi and K. K. Saxena, "Deformation Analysis of Al Alloy AA2024 through Equal Channel Angular Pressing for Aircraft Structures,"Advances in Materials and Processing Technologies, vol. 8, no. 1, pp. 828–842, 2022, https://doi.org/10.1080/2374068X.2020.1834756

[13] X. Guo, L. Meng and Y. Deng, "In-Situ EBSD Study on the Effect of Aging Conditions on Deformation Coordination of Grain Boundaries in Al-Cu-Li Alloys,"*Metallurgical and Materials Transactions A*, vol. 56, no. 3, pp. 865–886, 2025, https://doi.org/10.1007/s11661-024-07634-y

[14] G. Cui, D. Y. Kim, D. Zu, G. Chai and S. E. Lee, "Interferometric Phase Intensity Nanoscopy (iPINE), Revealing Nanostructural Features, Resolves Proximal Nanometer Objects below the Diffraction Limit: Implications in Long-Time Super-Resolution of Biological Dynamics,"*ACS Applied Nano Materials*, vol. 7, no. 16, pp. 18443–18449, 2024, https://doi.org/10.1021/acsanm.3c04361

[15] H. Yang, R. Huang, Y. Zhang, S. Zheng, M. Li, K. Sivasankar, K. Patiya and S. Janardan, "Effect of Rolling Deformation and Passes on Microstructure and Mechanical Properties of 7075 Aluminum Alloy,"*Ceramics International*, vol. 49, no. 1, pp. 1165–1177, 2023, https://doi.org/10.1016/j.ceramint.2022.09.093

[16] E. Yarar, A. T. Erturk and S. Karabay, "Dynamic Finite Element Analysis on Single Impact Plastic Deformation Behavior Induced by SMAT Process in 7075-T6 Aluminum Alloy,"*Metals and Materials International*, vol. 27, no. 8, pp. 2600–2613, 2021, https://doi.org/10.1007/s12540-020-00951-y

[17] A. Awasthi, U. S. Rao, K. K. Saxena and R. K. Dwivedi, "Impact of Equal Channel Angular Pressing on Aluminium Alloys: An Overview,"*Materials Today: Proceedings*, vol. 57, no. 7, pp. 908–912, 2022, https://doi.org/10.1016/j.matpr.2022.03.037

[18] M. Ren, S. Zhao, S. Gao, T. Zhang, M. Hou, W. Zhang, K. Feng, J. Zhong, W. Hua, S. Indris, K. Zhang, J. Chen and F. Li, "Homeostatic Solid Solution in Layered Transition-Metal Oxide Cathodes of Sodium-Ion Batteries,"Journal of the American Chemical Society, vol. 145, no. 1, pp. 224–233, 2022, https://doi.org/10.1021/jacs.2c09725

[19] N. Sharma, L. S. Vasconcelos, S. Hassan and K. Zhao, "Asynchronous-to-Synchronous Transition of Li Reactions in Solid-Solution Cathodes,"*Nano Letters*, vol. 22, no. 14, pp. 5883–5890, 2022, https://doi.org/10.1021/acs.nanolett.2c01818

[20] E. Spagnoli, A. Gaiardo, B. Fabbri, M. Valt, S. Krik, M. Ardit, G. Cruciani, M. D. Ciana, L. Vanzetti, G. Vola, S. Gherardi, P. Bellutti, C. Malagu and V. Guidi, "Design of A Metal-Oxide Solid Solution for Sub-Ppm H2 Detection,"*ACS Sensors*, vol. 7, no. 2, pp. 573–583, 2022, https://doi.org/10.1021/acssensors.1c02481

[21] A. Awasthi, A. Gupta, K. K. Saxena, R. K. Dwivedi, D. Kundalkar, D. S. Abdul-Zahra, A. Joshi and H. S. Saggu, "Design and Analysis of Equal-Channel Angular Pressing of Al6061: A Comparative Study,"*Advances in Materials and Processing Technologies*, vol. 10, no. 2, pp. 408–417, 2024, https://doi.org/10.1080/2374068X.2022.2134419

https://doi.org/10.64486/m.65.1.8